EXTENDED EXPERIMENTAL PROCEDURES

Plasmid Constructs

The following previously published DNA constructs were used in this study: Mito-DsRed, pEGFP-N1 (Clontech, Mountain View, CA), Synaptophysin-CFP (Seidl and Rubel, 2010), eGFP-OGT (Yang et al., 2008), nucleocytoplasmic OGT (Kreppel et al., 1997), Xpress-hMilton1 (OIP106/TRAK1) (Iyer et al., 2003), KHC-mCit (Cai et al., 2007), shRNA against OGT (Caldwell et al., 2010), myc-hMiro1 and 2 (Fransson et al., 2006), fly MiltonA truncated pieces (1-450,1-750,750-1116) and full length (Glater et al., 2006; Stowers et al., 2002), pcDNA3.1 FLII^{12}Pglu-700μδ6 (also called FLII^{12}Pglu-600μδ6, Addgene plasmid 17866) (Bittner et al., 2010; Takanaga et al., 2008; Tantama et al., 2012), RFP-Rab7 (Addgene plasmid 14436). shRNA against mouse Milton1 was purchased from Sigma MISSION shRNA library (TRC shRNA 0000126989). HA-hMiro1 and 2 were PCR amplified from myc-hMiro1/2 into Xho1/Xba1 sites of pCDNA3.HA vector (gift of K.J. Verhey). The following regions of hMilton1, containing the indicated amino acids, were PCR amplified from Xpress-hMilton1 and ligated into the BamHI/XhoI sites of the pCMV-Tag3A-myc vector (Agilent Technologies, Inc., Santa Clara, CA, USA): 1-350, 1-483, 483-953, 633-953. hMilton1 *O*-GlcNAcylation site mutants (S447A,S829A,S830A,S938A) and deletions (Δ658-672, Δ658-681, Δ771-859); OGT lacking TPR repeats (Δ2.5, Δ6), catalytic domain mutant (H498N) and shRNA-resistant OGT were generated using the QuikChange site-directed mutagenesis kit (Stratagene, Agilent Technologies, Inc., La Jolla, CA, USA).

Immunoreagents

For immunocytochemistry of COS7 cells and hippocampal neurons the following primary antibodies were used: anti-OGT at 1:200 (DM-17, Sigma-Aldrich), anti-GFP at 1:200 (Aves Labs, Inc.), anti-myc at 1:100 (9E10, Santa Cruz Biotechnology, Inc. or Novus Biologicals), anti-Tom20 at 1:200 (FL-145, Santa Cruz Biotechnology, Inc.), anti-GLUT3 at 1:200 (I-14, Santa Cruz Biotechnology, Inc.). The following fluorescently tagged secondary antibodies were used: Fluorescein anti-chicken at 1:500 (Aves Labs, Inc.), Alexa-647 or −568 conjugated anti-mouse and anti-rabbit at 1:500 (Molecular Probes, Invitrogen). Nuclei staining of COS7 cells were performed with Hoechst 33342 (Vybrant Apoptosis Assay Kit #5, Molecular Probes, Invitrogen) according to the protocol provided by the manufacturer.

The following primary antibodies were used for probing blots: anti-KHC at 1:2000 (clone H2, Millipore), anti-actin at 1:2000 (clone AC-74, Sigma-Aldrich), anti-*O*-GlcNAc at 1:2000 (RL-2, abcam), anti-HA at 1:2000 (clone 3F10, Roche Applied Science), anti-GAPDH at 1:5000 (clone 6C5, Millipore), anti-tubulin at 1:2000 (clone DM1A, Sigma-Aldrich), anti-Miro (RHOT1) at 1:2000 (clone 4H4, Sigma-Aldrich), anti-hMilton1(TRAK1) at 1:2000 (Sigma-Aldrich), anti-GFP at 1:2000 (Life Technologies), anti-myc at 1:500 (9E10), anti-OGT at 1:2000 (DM-17), anti-OGT at 1:2000 (H-300, Santa Cruz Biotechnology, Inc. for the detection of *Drosophila* OGT), anti-flyMiltonA 5A124 and 2A108 at 1:50 (Glater et al., 2006; Stowers et al., 2002). HRP-conjugated anti-mouse, rabbit and rat at 1:5000 (Jackson ImmunoResearch Laboratories, Inc.) secondary antibodies were used for enhanced chemiluminescent detection with SuperSignal West Dura (Pierce Biotechnology,Thermo Scientific). For detection of shorter pieces of flyMiltonA (Figure 4A) and hMilton1 (Figure S4B), mouse TrueBlot-HRP (eBioscience, Inc.) was used to avoid the strong signal from the IgG bands. For quantitative Western blots, CyDye (Cy2, 3 and 5) conjugated anti-mouse and rabbit secondary antibodies at 1:5000 (GE Healthcare, Life Sciences) were used to scan by a Typhoon Trio Image Scanner (Amersham BioSciences, Piscataway, NJ).

Verification of shRNA Constructs

We first confirmed the knockdown efficiency of the OGT shRNA constructs (a kind gift of M.J. Reginato) (Caldwell et al., 2010) against rat OGT by coexpressing rat eGFP-OGT (Yang et al., 2008) for 3-4 days in HEK293T cells and then measuring the level of GFP signal from cell lysates (Figure S2H). After confirming ~50% rat OGT knockdown efficiency, we further characterized the OGT shRNA constructs for endogenous OGT in rat primary neuron cultures. Rat hippocampal neurons were transfected with either scrambled or OGT shRNA constructs together and Mito-DsRed. Because the half-life of OGT protein was estimated to be ~13hours (Marshall et al., 2005), we expressed shRNA constructs in rat neurons for 4 days to achieve efficient knockdown of endogenous OGT. The efficiency of rat OGT knockdown was verified by immunocytochemistry using an antibody against endogenous OGT retrospectively (Figure S2G) for each transfection. The specificity of the OGT shRNA construct was verified by co-expressing an shRNA-resistant OGT construct with silent base mutations (Figures S2I and S2J).

For the msMilton1 knockdown experiments, we screened 5 different shRNA construct, designed by Sigma MISSION shRNA library, based on the mitochondrial phenotypes reported by van Spronsen et al. (2013). The most effective shRNA construct (TRC shRNA 0000126989) was selected for lentiviral particle production (Lois et al., 2002) and subsequently used to examine by immunoblotting the knockdown efficiency of the construct in neurons (Figure S5K). We expressed this shRNA constructs in mouse neurons for 3 days to achieve efficient knockdown of endogenous msMilton1 and arrest of mitochondrial motility, which could be rescued by shRNA insensitive hMilton1 constructs (Figure S5J).

Neuron Treatments

Glucose: Neuronal cultures were established with regular NB medium containing 25 mM glucose, unless otherwise indicated. Glucose levels were manipulated as shown in Figure 1A. For 5 mM or 1 mM glucose cultures, the requisite proportion of 0 mM glucose NB medium was mixed with 25 mM glucose NB medium to avoid osmolarity changes. To obtain 30 mM glucose, 25 mM glucose NB medium was supplemented with D-glucose (Sigma-Aldrich). An osmolarity effect was ruled out by using the

same amount of D-mannitol (Sigma-Aldrich). To generate a glucose gradient, neurons were cultured in microfludic devices (see Extended Experimental Procedures). For the experiment sets with 1 mM or 0 mM glucose, NB medium was supplemented with 1 mM lactate (Sigma) and 1 mM pyruvate (Cellgro). 0 mM glucose HibernateE was custom ordered to match the imaging medium to the culture conditions. To obtain 30 mM glucose, 25 mM glucose HibernateE medium was supplemented with D-glucose. To determine the changes in intracellular glucose concentration, real-time glucose flux in neurons was measured by expressing FLII^{12}Pglu-600μδ6, a fluorescent glucose sensor, in neurons (see Extended Experimental Procedures).

PUGNAC: OGA inhibitor, PUGNAC (Tocris Bioscience) was applied at 100μM for 6 hr before live cell imaging.

DON and Glucosamine: For the long-term DON applications (3 days), neurons were transfected with the indicated constructs (Figure S2). Immediately after, the GFAT inhibitor DON (Sigma) treatments were applied at 10μM for 72 hr before live cell imaging. Medium containing 10μM DON was refreshed every 24 hr throughout the treatment.

To test whether inhibition of GFAT with DON blocked the inhibitory effect of elevated glucose on mitochondrial motility, neurons were pretreated with 100μM DON 1h before and 2 hr with the glucose challenge. To bypass GFAT inhibition, instead of elevating the glucose level, neurons were treated with 4 mM Glucosamine (Sigma) in 1 mM glucose NB (Figures 2I–2M).

The same amount of vehicle treatment was included as a negative control for each data set. All treatments were kept constant in the live cell imaging medium Hibernate E to match to the culture conditions.

Neuronal Cultures in Microfludic Devices

Rat hippocampal neurons were plated at a density of 5x10^6/cm^2 on the somal side of microfluidic devices based on the non-plasma bonding protocol provided by the manufacturer (Xona Microfluidics LLC) (Taylor et al., 2005). Neuronal cultures were established with NeuroBasal medium, containing 5 mM glucose, 1 mM lactate and 1 mM pyruvate. The medium was refreshed every 24 hr throughout both in somal and axonal compartments. Neurons were transfected with Mito-DsRed at 10DIV and a 50 μm stretch of axon was imaged at 12DIV (Figure 7G). Hibernate E (BrainBits) containing either 5 mM or no glucose with 1 mM lactate and 1 mM pyruvate was used as an imaging medium. Images were acquired by a spinning disk inverted confocal microscope (Perkin Elmer Ultraview Vox), equipped with an environmental chamber and with Volocity software and using a 40x objective. First, the 50 μm portion of an axon adjacent to the axonal compartment was imaged, while both the somal and axonal compartments were in 5 mM glucose. Afterward, the imaging medium in the somal compartment was replaced with either 5 mM or glucose-free medium, while the axonal compartment was kept at 5 mM glucose and the same axonal area was imaged 1h later. The Trypan blue (Sigma) was used to test fluidic isolation of the axonal compartment during medium changes. Mitochondrial density and length were measured for each axon and changes in the ratios of those parameters before and after the medium change were quantified.

Intracellular Glucose Measurements

To determine whether the shift in extracellular glucose changed intracellular glucose concentrations in neurons, real-time intracellular glucose was measured by live cell imaging of neurons expressing FLII^{12}Pglu-600μδ6, a fluorescent glucose-sensor (Bittner et al., 2010; Hou et al., 2011). Time-lapse movies were acquired on a Zeiss LSM 510 confocal microscope equipped with a temperature-controlled stage (PeCon GmbH, Erbach, Germany) at 37°C and with a 63 × /N.A. 0.90 water IR-Achroplan objective. Hibernate E imaging medium was used with the indicated glucose concentrations. Images were acquired for each experimental point by using a 458nm laser for excitation and dual emission at 470nm and 535nm. The ratio of the two channels in the selected region of interest for each neuron was quantified with Image J (developed by Wayne Rasband).

O-GlcNAcylation Measurements

HEK293T cells were plated at 6x10^5 cells/well density in a 6-well plate and transfected with the indicated plasmid constructs the next day. Three days after reaching confluency, cells were washed once with ice-cold phosphate-buffered saline (PBS) containing 1 μM PUGNAC and lysed in 600μl buffer containing: 1% Nonidet P-40 (Calbiochem, San Diego, CA, USA), 15 mM Tris-HCl (pH 7.5), 150 mM NaCl, 1 mM EDTA, 40 mM GlcNAc, 1 μM PUGNAC, (Sigma-Aldrich, Saint Louis, MO), 1 mM DTT (GBiosciences), 0.1 mg/ml PMSF and protease inhibitor cocktail (Calbiochem, San Diago, CA, USA) at 1:1000. Lysates were centrifuged 10 min at 13,000 x *g* at 4°C and the supernatants were collected. For immunoprecipitations of myc-hMilton1 WT or GlcNAc site mutants, 1.2 μg anti-myc or anti-TRAK1 antibody, as indicated, incubated for 2 hr at 4°C with 500 μl of whole-cell lysates, then 1 more hour with protein-A-Sepharose beads. Beads were washed three times with lysis buffer and resuspended with 1xLaemmli buffer. 80%–90% of immunoprecipitates were separated by SDS-PAGE and transferred to nitrocellulose membranes. For GlcNAcylation measurements, blots were first incubated with blocking buffer containing 3% bovine serum albumin (w/v) in Tris-buffered saline 0.1% Tween20 (Sigma-Aldrich, Saint Louis, MO) then probed with anti-GlcNAc antibody overnight (Whelan et al., 2008). For quantitative immunodetection of the GlcNAc signal, Cy5 conjugated secondary antibody was used at 1:5000. The same blot was reprobed with anti-myc or anti-TRAK1 antibody after washing thoroughly and blocking with 5% non-fat dry milk in PBS for 1-2 hr at room temperature. For quantitative immunodetection, Cy2 conjugated secondary antibody was used at 1:5000. Blots were scanned by a Typhoon Trio Image Scanner (Amersham BioSciences, Piscataway, NJ). Image acquisition settings were changed to keep the fluorescent signal within the linear range. The ImageJ gel analyzer function was used to analyze the fluorescence intensity of each band.

To measure the dependence of Milton GlcNAcylation on extracellular glucose, HEK293T cells were plated at 6x10^5 cells/well in a 6-well plate, cultured in 25 mM glucose DMEM and transfected with the indicated plasmid constructs on the following day together

with GLUT2 to ensure glucose uptake (Hou et al., 2011). A day after the transfection, the culture medium was switched to 5 mM DMEM for 24 hr before challenging the cells with 30 mM or 5 mM glucose for 2 hrs. Following the glucose treatments, cells were washed once with ice-cold phosphate-buffered saline (PBS) containing 1 μM PUGNAC and processed as described above.

Fasting/Refeeding Studies in Mice

Age matched (8-weeks old) male C57Bl/6J mice were housed at 22-24°C using a 12h light/12h dark cycle with ad libitum access to standard mouse chow and water. Care of animals and diet change procedures was approved by the Beth Israel Deaconess Medical Center Institutional Animal Care and Use Committee. For fasting and refeeding studies, food was removed, and then replaced 24 hr later. The manipulations in diet and blood glucose measurements were matched to the start of the ''lights-on'' cycle. Blood was sampled from the tail vein, and glucose levels were measured with a glucometer (Onetouch Ultra 2). To measure Milton *O*-GlcNAcylation, immediately after the blood glucose measurements, two hemispheres of brain cortexes were dissected and placed in ice-cold PBS containing 1 μM PUGNAC. Brains were homogenized in lysis buffer (10% wt/vol), centrifuged at 16,000 g for 15 min at 4°C and msMilton1 immunoprecipitated with Milton1 antibody as described above.

Mass Spectrometry Analysis

Myc-hMilton1 immunoprecipitated from HEK293T cells as described above. To maximize the GlcNAcylation levels on hMilton1, cells were treated with 100 μM PUGNAC overnight. ''SimpleBlue Safestain'' (Invitrogen, Carlsbad, CA) stained gel band corresponding to myc-hMilton1 (as well as the control lane) were excised and minced. Samples were analyzed by mass spectrometry as described previously (Trinidad et al., 2012).

Live-Image Acquisition and Quantification

Time-lapse movies were acquired on a Zeiss LSM 510 confocal microscope equipped with a temperature-controlled stage (PeCon GmbH, Erbach, Germany) at 37°C and with a 63 × /N.A. 0.90 water IR-Achroplan objective. Images were captured every 2-9 s. as previously described (Wang and Schwarz, 2009b). Laser power was set to < 20% for each channel to minimize damage. Pinholes were opened > 5μm to allow the entire thickness of the axon to be imaged. 100-150 μm of axon, at least 250 μm away from the cell body and generally closer to the axon terminal were selected for analysis. Mitochondrial and Synaptophysin (Syp) vesicle motility was examined in cultured rat hippocampal neurons sparsely transfected with Mito-DsRed and Syp-CFP. We restricted our analysis to neuronal axons, which have a uniform microtubule polarity with (+)-ends directed distally (Baas et al., 1988), and identified them either by co-transfection with the axonal marker Syp-CFP or by morphological criteria when Mito-DsRed was transfected alone (Chang et al., 2006). Time lapse movies were acquired as described in the Experimental Procedures with LSM software 3.2 (Carl Zeiss Microimaging Inc.) and analyzed with ImageJ (developed by Wayne Rasband) extended with the MBF plugin collection (organized by Tony Collins at the McMaster Biophotonics Facility), ''LSM toolbox'' (developed by Patrick Pirrotte, Jérome Mütterrer) and ''Path Writer'' plugins (Schneider et al., 2012). A custom-made Image J macro ''Kymolyzer'' was developed based on previously described codes (De Vos and Sheetz, 2007) for kymograph based motility analysis. Briefly, selected axons were thresholded using Otsu's algorithm, the center of mass was highlighted and maximal projection was performed to identify the particle's (mitochondria or vesicles) paths. The segmented line tool was used to manually draw a line along the particle trajectories and calibrated (time in seconds across the y axis and distance in μm along the x axis) kymographs were generated from the region of interest. For Syp and Rab7 movies, a smooth function was applied to reduce the noise when necessary before generating the kymographs. Mitochondria length/density measurements were performed by using the first frame of the each time lapse recording in selected axons. Kymographs were then analyzed by manually tracing individual particles. The ''maximum finder'' function was applied and a reference point for each particle was highlighted to avoid personal bias during the tracing. The tracked particle was also automatically marked in the original video recording to further confirm the tracing before extracting the parameters. Motility parameters were calculated at a spatial and temporal resolution of 0.4 μm and 0.3 Hz respectively. Velocities less than 0.05 μm/sec were considered zero to avoid bias caused by stage drift (Wang and Schwarz, 2009b). The average velocity of all instantaneous velocities that are not zero for a mitochondrion is defined as the ''Average Velocity.'' The percent time each mitochondrion spent in motion was calculated by averaging the total numbers of instantaneous velocities (including both zero and non-zero) for each mitochondrion. ''Total Distance Travelled'' was defined as the average of total distances traveled for each mobile mitochondrion. Calculations from ImageJ were extracted as excel spreadsheets (Microsoft Excel) and statistical analysis was performed with GraphPad Prism version 6.0 for Mac OS X (GraphPad Software, Inc., La Jolla, CA, USA).

SUPPLEMENTAL REFERENCES

Baas, P.W., Deitch, J.S., Black, M.M., and Banker, G.A. (1988). Polarity orientation of microtubules in hippocampal neurons: uniformity in the axon and nonuniformity in the dendrite. Proc. Natl. Acad. Sci. USA *85*, 8335–8339.

Bittner, C.X., Loaiza, A., Ruminot, I., Larenas, V., Sotelo-Hitschfeld, T., Gutierrez, R., Cordova, A., Valdebenito, R., Frommer, W.B., and Barros, L.F. (2010). High resolution measurement of the glycolytic rate. Front Neuroenergetics *2*, 26.

Cai, D., Hoppe, A.D., Swanson, J.A., and Verhey, K.J. (2007). Kinesin-1 structural organization and conformational changes revealed by FRET stoichiometry in live cells. J. Cell Biol. *176*, 51–63.

De Vos, K.J., and Sheetz, M.P. (2007). Visualization and quantification of mitochondrial dynamics in living animal cells. Methods Cell Biol. *80*, 627–682.

Fransson, S., Ruusala, A., and Aspenström, P. (2006). The atypical Rho GTPases Miro-1 and Miro-2 have essential roles in mitochondrial trafficking. Biochem. Biophys. Res. Commun. *344*, 500–510.

Kreppel, L.K., Blomberg, M.A., and Hart, G.W. (1997). Dynamic glycosylation of nuclear and cytosolic proteins. Cloning and characterization of a unique O-GlcNAc transferase with multiple tetratricopeptide repeats. J. Biol. Chem. *272*, 9308–9315.

Lois, C., Hong, E.J., Pease, S., Brown, E.J., and Baltimore, D. (2002). Germline transmission and tissue-specific expression of transgenes delivered by lentiviral vectors. Science *295*, 868–872.

Marshall, S., Okuyama, R., and Rumberger, J.M. (2005). Turnover and characterization of UDP-N-acetylglucosaminyl transferase in a stably transfected HeLa cell line. Biochem. Biophys. Res. Commun. *332*, 263–270.

Renò, F., Falcieri, E., Luchetti, F., Burattini, S., and Papa, S. (1997). Discrimination of apoptotic cells in flow cytometry using trypan blue and FDA. Eur. J. Histochem. *41* (*Suppl 2*), 115–116.

Seidl, A.H., and Rubel, E.W. (2010). A simple method for multiday imaging of slice cultures. Microsc. Res. Tech. *73*, 37–44.

Takanaga, H., Chaudhuri, B., and Frommer, W.B. (2008). GLUT1 and GLUT9 as major contributors to glucose influx in HepG2 cells identified by a high sensitivity intramolecular FRET glucose sensor. Biochim. Biophys. Acta *1778*, 1091–1099.

Tantama, M., Hung, Y.P., and Yellen, G. (2012). Optogenetic reporters: Fluorescent protein-based genetically encoded indicators of signaling and metabolism in the brain. Prog. Brain Res. *196*, 235–263.

Taylor, A.M., Blurton-Jones, M., Rhee, S.W., Cribbs, D.H., Cotman, C.W., and Jeon, N.L. (2005). A microfluidic culture platform for CNS axonal injury, regeneration and transport. Nat. Methods *2*, 599–605.

Whelan, S.A., Lane, M.D., and Hart, G.W. (2008). Regulation of the O-linked beta-N-acetylglucosamine transferase by insulin signaling. J. Biol. Chem. *283*, 21411–21417.

Yang, X., Ongusaha, P.P., Miles, P.D., Havstad, J.C., Zhang, F., So, W.V., Kudlow, J.E., Michell, R.H., Olefsky, J.M., Field, S.J., and Evans, R.M. (2008). Phosphoinositide signalling links O-GlcNAc transferase to insulin resistance. Nature *451*, 964–969.

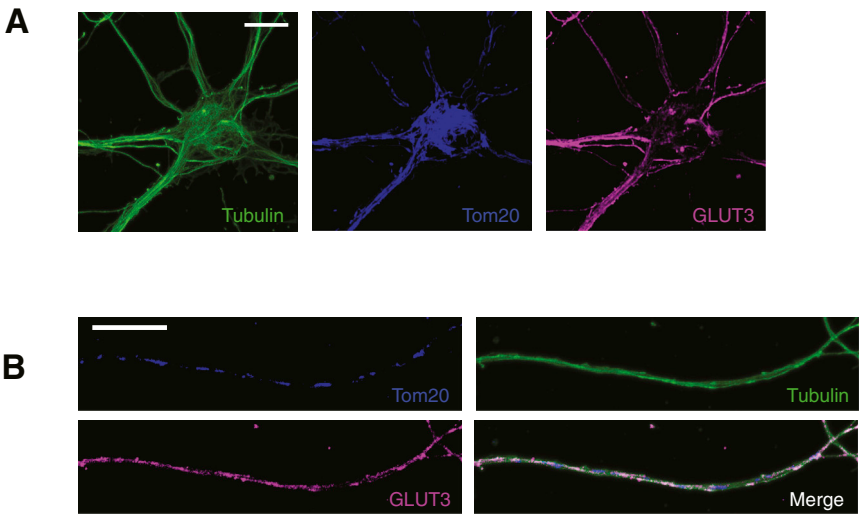

Figure S1. Cellular Localization of Neuronal Glucose Transporter (GLUT3), Related to Figure 1

(A and B) Rat hippocampal neuron cultures were immunostained with anti-GLUT3 (magenta), anti-tubulin(green) and the mitochondrial marker anti-Tom20 (blue). GLUT3 immunoreactivity is present in neuronal cell bodies (A) and in densely spaced patches along the neuronal processes (B). The widespread distribution of the transporter makes it likely that all the mitochondria in the processes are in the vicinity of transporters. Scale bar, 10 μm.

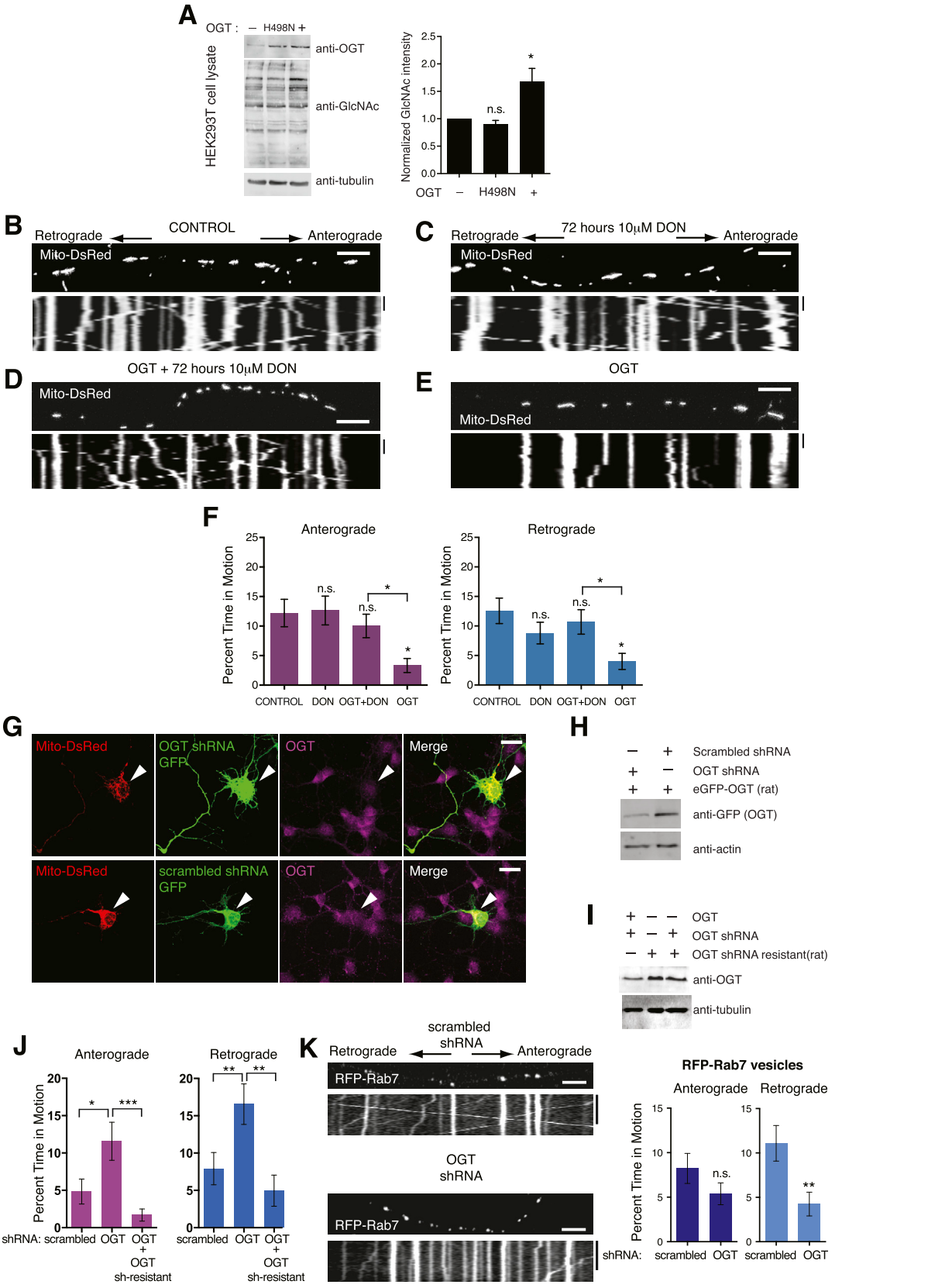

(legend on next page)

Figure S2. Regulation of Mitochondrial Motility by OGT and the Hexosamine Biosynthetic Pathway, Related to Figure 2

(A) Protein *O*-GlcNAcylation in HEK293T cells is increased by expression of OGT but not catalytically dead OGT (OGTH498N). Cell lysates were separated by SDS gel electrophoresis and probed with anti-*O*-GlcNAc, anti-OGT, and anti-tubulin as a loading control. The total intensity of the GlcNAc immunoreactive bands was normalized to the intensity of the tubulin band for that lane. The amount of GlcNAc immunoreactivity in untransfected cells was set as 1 and fold changes were calculated. $n \geq 3$ independent transfections per condition.

(B–E) Hippocampal neurons, cultured in 5 mM glucose, were transfected with Mito-DsRed either with (D and E) or without (B and C) OGT and mitochondrial motility imaged 3 days later. Representative kymographs are shown. The GFAT inhibitor 10μM DON was used in (C) and (D) to block synthesis of UDP-GlcNAc. DON was refreshed every 24 hr throughout the treatment.

(F) Mitochondrial motility was quantified from kymographs as in (B - E) and compared with control. n = 114-151 mitochondria from 8 axons and 4 independent transfections per condition.

(G) Knockdown of endogenous neuronal OGT by shRNA. Hippocampal neurons were transfected with Mito-DsRed (red) and a vector containing GFP (green) and either a scrambled shRNA or OGT shRNA. 4 days after the transfection, neurons expressing the indicated constructs were fixed and immunostained with anti-OGT antibody (magenta). Image acquisition settings were adjusted to avoid saturation of the signal in the cell bodies and therefore the signals in most neuronal processes are not visible. Arrowheads indicate the cell body of a neuron expressing the indicated constructs. n = 3 independent transfections per condition. Scale bar, 20 μm.

(H) HEK293T cells were transfected with a rat eGFP-OGT construct to test the knock-down efficiency of OGT shRNA constructs against rat OGT. Cell lysates were probed with anti-GFP and anti-actin was used as a loading control.

(I) HEK293T cells were transfected shRNA-resistant rat OGT construct with and without with OGT shRNA to test the insensitivity of this OGT construct to shRNA. Cell lysates were probed with anti-OGT and anti-tubulin was used as a loading control.

(J) Hippocampal neurons were transfected with Mito-DsRed (red) and a vector containing GFP (green) and OGT shRNA or scrambled shRNA either with or without shRNA-resistant OGT. 4 days after the transfection, mitochondrial motility in neurons expressing the indicated constructs was analyzed. n = 70-106, 7 axons and 2 independent transfections.

(K) Hippocampal neurons were transfected with RFP-Rab7 and a vector containing GFP (green) and OGT shRNA or scrambled shRNA. RFP-Rab7 vesicles motility was quantified from kymographs. n = 109-115 vesicles from 8 axons and 3 independent transfections per condition.

All values are shown as mean ± SEM n.s. not significant. *$p < 0.05$, **$p < 0.01$, ***$p < 0.001$; Kruskal-Wallis test or Mann-Whitney *U* test. Scale bar, 10 μm and 100 s.

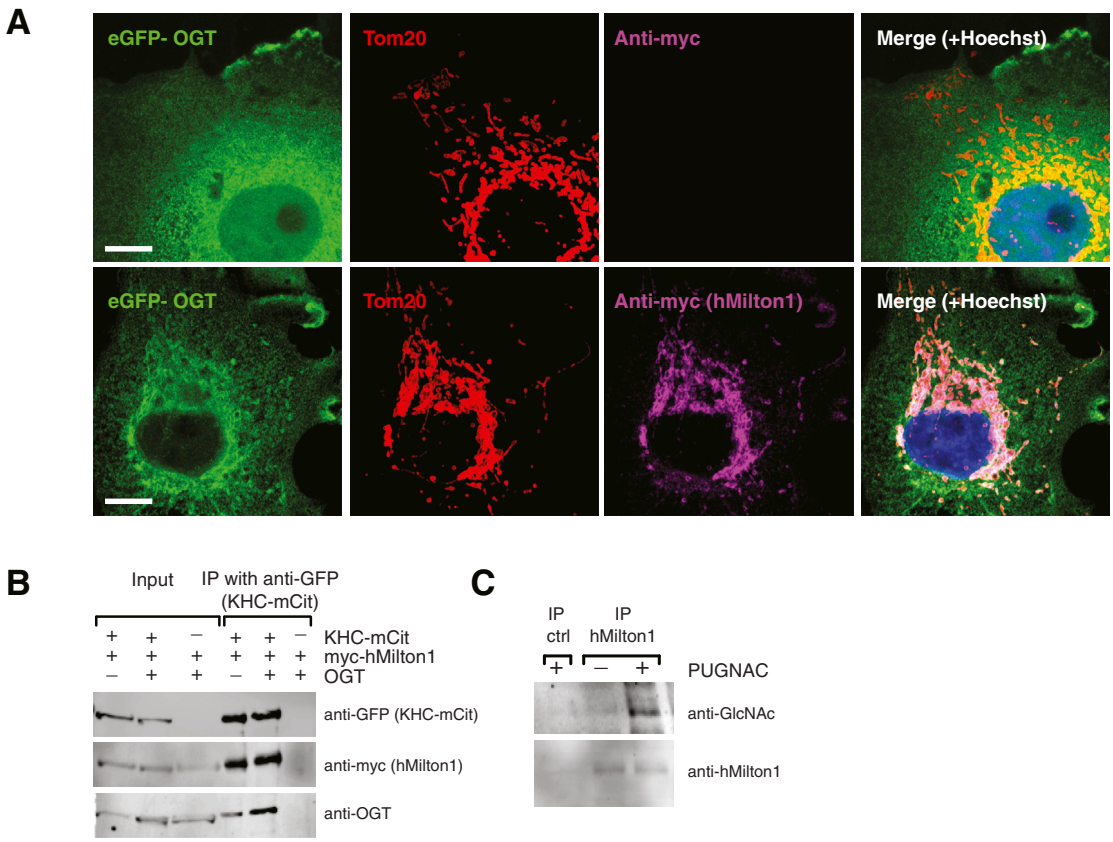

Figure S3. hMilton1 Recruits OGT to the Mitochondrial Motor/Adaptor Complex, Related to Figure 3

(A) COS7 cells were transfected with eGFP-OGT and either empty vector or myc-hMilton1. Cells were immunostained with the mitochondrial marker anti-Tom20 (red), anti-GFP (green) and anti-myc (magenta) antibodies. The presence of myc-hMilton1 caused the otherwise diffuse OGT to concentrate on mitochondria.

(B) HEK293T cells were transfected with KHC-mCit and myc-hMilton1, and either with or without OGT. KHC-mCit was immunoprecipitated with anti-GFP antibody and probed with anti-GFP, myc and OGT antibodies. Both Milton and OGT coprecipitated with KHC.

(C) HEK293T cells were cultured overnight with or without 100 μM PUGNAC. Endogenous hMilton1 immunoprecipitated with anti-Milton1 antibody and probed with anti-GlcNAc and anti-hMilton1 antibodies. PUGNAC treatment increases *O*-GlcNAcylation of endogenous hMilton1.

n = 3 independent transfections per condition. Scale bar, 10 μm.

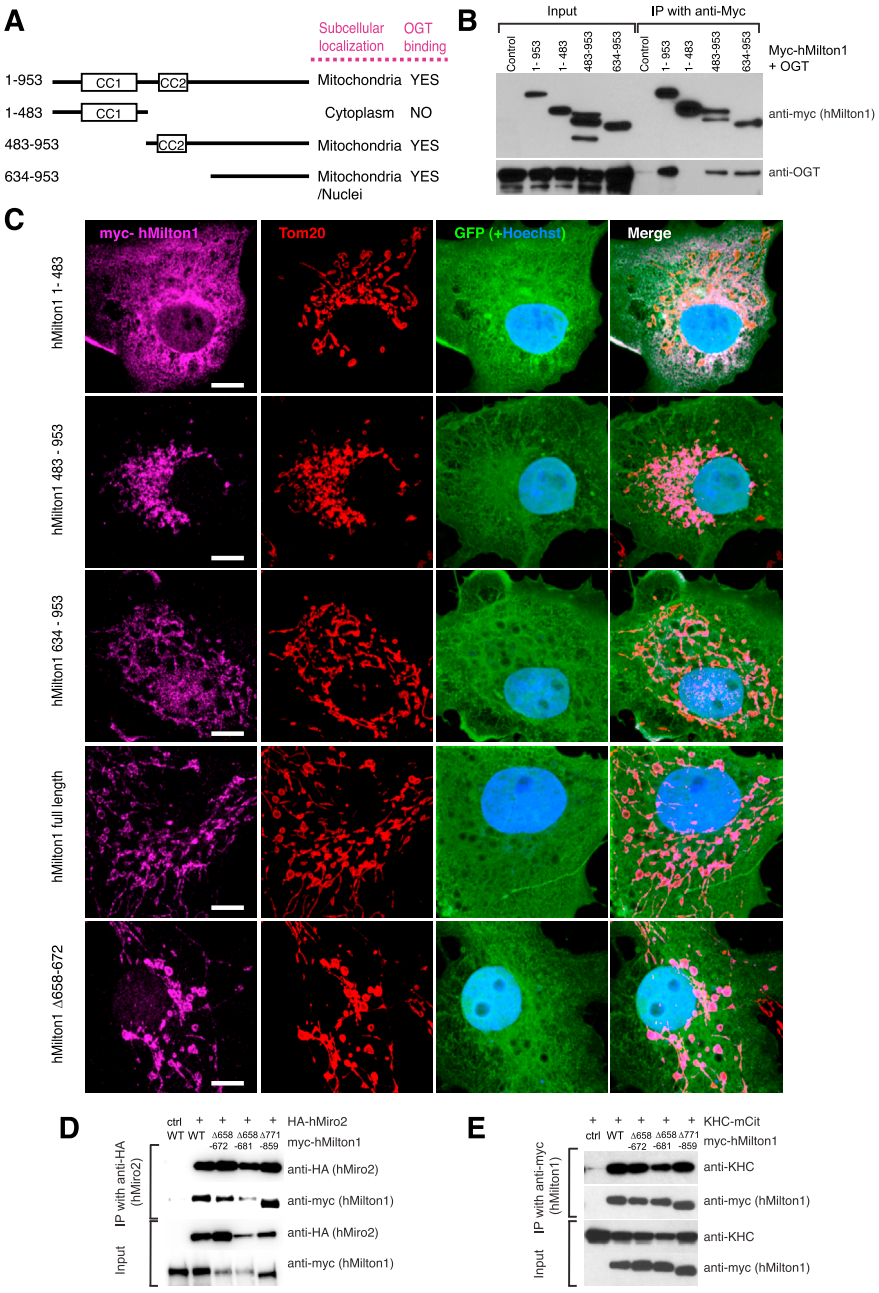

Figure S4. Mapping and Characterization of the OGT-Binding Domain in hMilton1, Related to Figure 4

(A) Schematic summary of N- and C-terminal truncated hMilton1 constructs, their subcellular localization and OGT binding efficiency. Predicted coiled coil domains (CC) 1 and 2 are indicated.

(B) Coimmunoprecipitation of full length or truncated hMilton1 and OGT from HEK293T cells. Cells were transfected as indicated and the myc-tagged hMilton1 proteins were immunoprecipitated with anti-myc antibody and assayed for OGT binding.

(C) COS7 cells were transfected with GFP and full length, truncated (as shown in A) or Δ658-672 (also named ΔOBD) hMilton1 constructs and immunostained with anti-myc (magenta), Tom20 (red) and Hoechst (blue) to identify their subcellular localizations.

(D) Coimmunoprecipitation of full length or deleted hMilton1 and Miro proteins from HEK293T cells. hMilton1 deletion constructs, lacking only the indicated amino acids, Δ658-672 (also named ΔOBD), Δ658-681 and Δ771-859 and full length myc-hMilton1 were expressed together with HA-Miro2 in HEK293T cells. Miro co-precipitated with each of the hMilton1 constructs.

(E) Coimmunoprecipitation of full length and deleted hMilton1 and KHC proteins from HEK293T cells. Myc-tagged hMilton1 deletion constructs were expressed together with KHC-mCit in HEK293T cells, immunoprecipitated with anti-myc, and assayed for KHC binding.

n ≥ 3 independent transfections per condition. Scale bar, 10 μm.

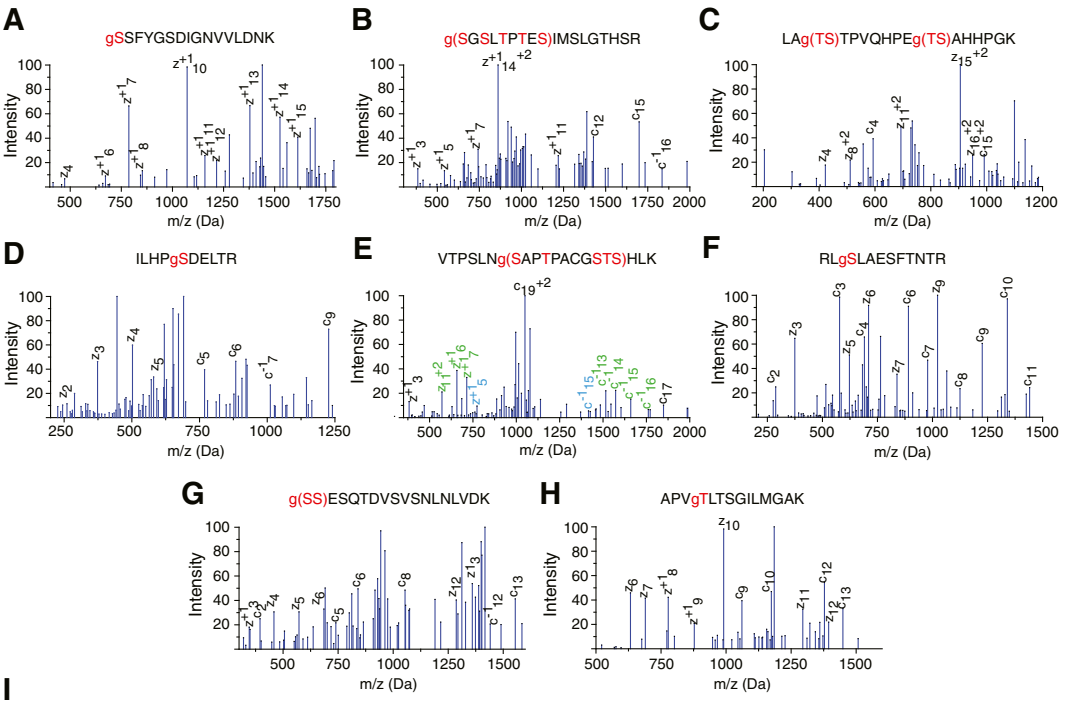

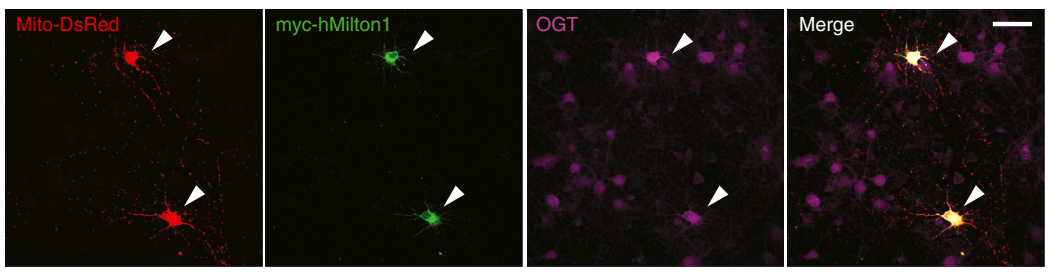

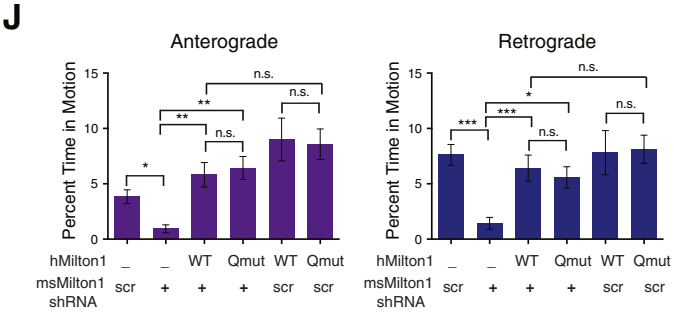

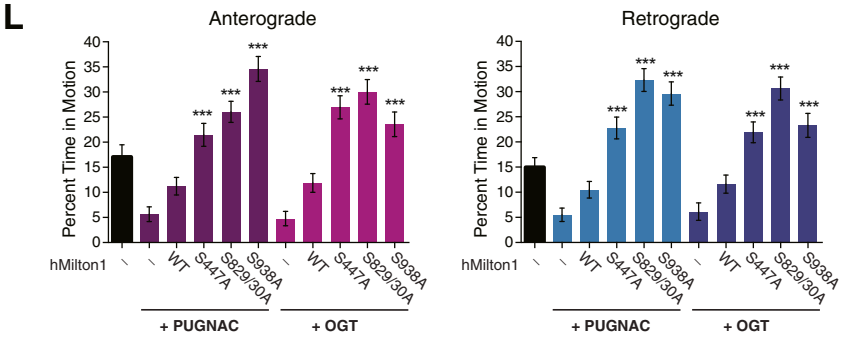

(legend on next page)

Figure S5. Identification and Functional Analysis of hMilton1 GlcNAcylation Sites, Related to Figure 5

(A–H) Tandem mass spectra showing O-GlcNAc on peptides derived from hMilton1. Data were acquired using ETD fragmentation and prominent c and z-type ions are labeled. The peptide shown in C was doubly GlcNAcylated. The spectrum in E showed fragment ions consistent with a GlcNAc toward the amino terminus (green) as well as ions consistent with a GlcNAc toward the carboxy terminus (blue), suggesting that multiple versions of this peptide were probably co-fragmented in the mass spectrometer. For clarity, the spectra in G and H were scaled to the height of the second most abundant peak.

(I) Retrospective immunostaining of neurons to examine the extent of co-expression. Hippocampal neurons were transfected with Mito-DsRed (red) and WT or GlcNAc site mutated hMilton1 and OGT constructs. After live cell imaging, neurons were fixed and immunostained with anti-OGT (magenta) and anti-myc (green) antibodies. Image acquisition settings were adjusted to avoid saturation of the signal in the cell bodies; therefore the signals in most neuronal processes are not visible. Arrowheads indicate the cell body of a neuron expressing all three constructs. For each transfection, 96 ± 2.27% of the cells that were positive for a single marker also expressed the other two.

(J) 4DIV Mouse hippocampal neurons were transfected with Mito-DsRed and either shRNA against endogenous mouse Milton1 or a scrambled shRNA. Three days after the transfection, mitochondrial motility in neurons expressing the indicated constructs was analyzed. The arrest caused by msMilton1 knockdown was rescued by co-transfecting neurons with shRNA-insensitive either hMilton1, either WT or Qmut. n = 90-351 mitochondria from 6-20 axons, n = 4 independent transfections.

(K) The efficiency of msMilton1 shRNA was further confirmed by generating lentiviral particles and infecting cortical neuronal cultures. Neuronal lysates were probed with anti-Milton1 and anti-tubulin was used as a loading control.

(L) Hippocampal neurons were transfected with Mito-DsRed and hMilton1 and OGT constructs, as indicated. Mitochondrial motility was imaged 3 days after the transfection. The indicated data sets were also treated with the OGA inhibitor PUGNAC. The percent time each mitochondrion spent in anterograde and retrograde motion was calculated from the kymographs. n = 109-185 mitochondria from 9-10 axons and 3 independent transfections per condition.

All values are shown as mean ± SEM n.s. not significant. *$p < 0.05$, **$p < 0.01$, ***$p < 0.001$; Kruskal-Wallis test, each GlcNAc site mutant was compared to WT hMilton1 within the data sets.

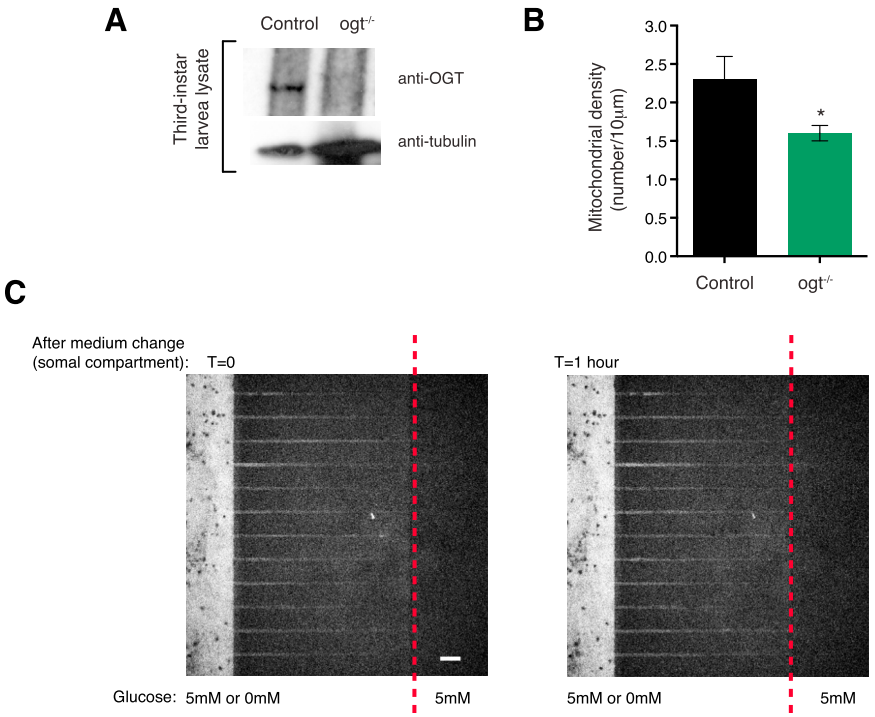

Figure S6. Characterization of *ogt*$^{-/-}$ *Drosophila* Larvae and of Fluidic Isolation in the Microfluidic Cultures, Related to Figure 7

(A) Lysates of WT or *ogt*$^{-/-}$ third-instar *Drosophila* larvae were probed with anti-OGT and anti-tubulin as a loading control. The absence of OGT immunoreactivity confirms the efficacy of the mutation.

(B) In control and ogt$^{-/-}$ larvae UAS-mito-GFP was expressed in an axon within the segmental nerve by CCAP-GAL4 to quantify mitochondrial motility (Figure 7) and, as shown here, density which was reduced in the mutants. n = 91-100 mitochondria from 9 axons from 9 animals. All values are shown as mean ± SEM. *p < 0.05; Mann-Whitney *U* test.

(C) Fluidic isolation of the axonal compartment, during our medium changes, was tested by using Trypan blue, which emits a red fluorescence (>620 nm) when, excited by a 488 nm laser (Renò et al., 1997). The medium was switched to dye-containing glucose-free medium and the microfluidic device was imaged immediately and an hour later.